Available online at www.sciencedirect.com

SciVerse ScienceDirect

Journal of the European Ceramic Society 32 (2012) 1925–1932

www.elsevier.com/locate/jeurceramsoc

Grain boundary glasses in silicon nitride: A review of chemistry, properties and crystallisation

Stuart Hampshire *, Michael J. Pomeroy

Materials and Surface Science Institute, University of Limerick, Limerick, Ireland

Available online 18 January 2012

Abstract

Silicon nitride for engineering applications is densified by liquid phase sintering using oxide additives such as yttria and alumina. The oxynitride liquid remains as an intergranular glass. This paper provides a review of microstructural development in silicon nitride, grain boundary oxynitride glasses and effects of chemistry on properties. Nitrogen increases T_g, viscosities, elastic moduli and microhardness. These property changes are compared with known effects of grain boundary glass chemistry in silicon nitride ceramics where significant improvements in fracture resistance of silicon nitride can be achieved by tailoring the intergranular glass chemistry.

Crystallisation of the grain boundary Y–Si–Al–O–N glass phase can improve properties. Nucleation and crystallisation of a Y–Si–Al–O–N glass, similar to that found in grain boundaries of silicon nitride densified with yttria and alumina, can be optimised to form different Y-disilicate polymorphs at different temperatures. One solution to provide a single disilicate phase over a range of temperatures is discussed.

Keywords: Si_3N_4; Sialon; Sintering; Grain boundaries; Mechanical properties; Thermal properties

1. Introduction – microstructural development in silicon nitride

Silicon nitride-based ceramics including SiAlONs are important structural materials that have been for many years the focus of extensive research effort.[1–12] These ceramics possess high flexural strength and fracture toughness, high hardness, excellent wear resistance and low creep deformation up to 1350 °C. These properties arise from the development of microstructures through the processing of the ceramic by liquid phase sintering[1–4] which results in full densification and formation of high aspect (length to diameter) ratio β-Si_3N_4 grains surrounded by a grain boundary glass phase leading to excellent fracture toughness and high strength.[8–12]

Sintering of silicon nitride is carried out at 1750–1900 °C under a nitrogen atmosphere (0.1–10 MPa). Sintering additives, such as yttria (or various lanthanide oxides) and alumina, are mixed with α-Si_3N_4 powder particles which possess surface layers of silica. The oxides react with this silica and some of the nitride itself at sintering temperatures to form an oxynitride liquid which promotes densification by solution–precipitation.[1–4]

The α → β transformation in silicon nitride requires a lattice reconstruction. This type of process occurs when the transforming material is in contact with a solvent, in this case a Y–Si–Al–O–N oxynitride liquid phase. The greater solubility of the less stable α form drives it into solution after which it precipitates as the less soluble, more stable β form in excess of 1400°C.[3,4]

A systematic study of pressureless sintering kinetics for silicon nitride ceramics[3,4] applied the Kingery liquid-phase sintering model[14] in which three stages are identified:

(1) *Particle Rearrangement* following formation of the initial liquid phase, where the rate and the extent of shrinkage depend on both the volume and the viscosity of the liquid; the volume depends on the total amount of oxide additives while the viscosity depends on additive (e.g. Y_2O_3:Al_2O_3) ratios; this stage is also the incubation period for the α → β transformation.[4]

(2) *Solution–diffusion–reprecipitation*, where, according to Kingery, shrinkage is given by:

$$\frac{\Delta V}{V_o} \propto t^{l/n} \tag{1}$$

where t is time and $n = 3$ if solution into or precipitation from the liquid is rate controlling,[3,4] as is the case for lower

* Corresponding author. Tel.: +353 61 202640; fax: +353 61 202967.
E-mail address: stuart.hampshire@ul.ie (S. Hampshire).

0955-2219/$ – see front matter © 2012 Elsevier Ltd. All rights reserved.
doi:10.1016/j.jeurceramsoc.2011.12.023

viscosity liquids with additives such as MgO or low Z lanthanide (Ln) oxides, and $n = 5$ if diffusion through the liquid is rate-controlling, as is the case for high Z lanthanide oxides, where diffusion through a more viscous oxynitride liquid is much slower.[4] The α → β transformation begins during this stage and proceeds by dissolution of α and precipitation of Si and N onto existing β grains, which grow in the longitudinal direction as prismatic hexagonal rod-like crystals that eventually impinge on each other forming an interlocked microstructure. With lower viscosity liquid phases, the transformation proceeds when densification is almost complete and is enhanced by high N solubility within the liquid phase.[4,10]

(3) *Coalescence* or elimination of closed porosity and grain growth, during which the liquid acts to promote further growth of the β grains but this critically depends on the liquid-phase composition, established by the additives used, and also the use of high α or high β content powders or β seeds, all of which have a significant impact on phase transformation, microstructural development and densification.[9–12] After cooling, the liquid remains as an intergranular phase, usually a glass, according to the following:

$$\alpha\text{-}Si_3N_4 + SiO_2 + Y_2O_3 + Al_2O_3 \rightarrow \beta\text{-}Si_3N_4 + \text{Y–Si–Al–O–N phase} \quad (2)$$

Fig. 1 shows a scanning electron micrograph of silicon nitride sintered with 6 wt.% yttria and 2 wt.% alumina[15] in which can be seen high aspect ratio β-Si_3N_4 grains surrounded by a Y–Si–Al–O–N grain boundary glass phase (white). For

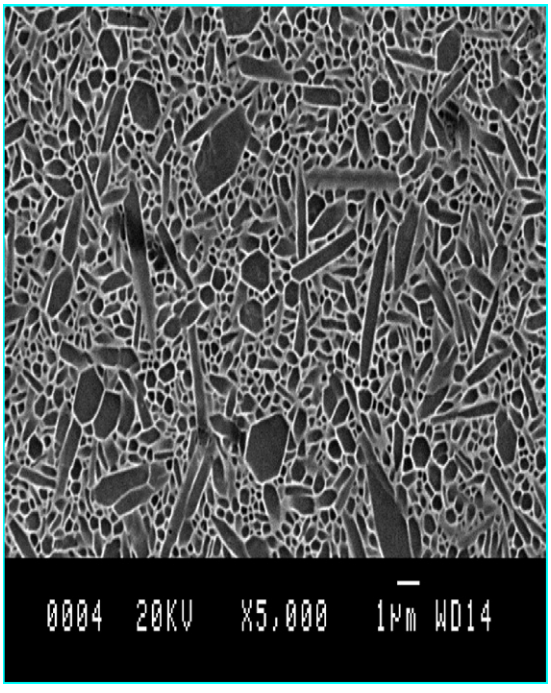

Fig. 1. Scanning electron micrograph of silicon nitride densified with 6 wt.% yttria and 2 wt.% alumina.

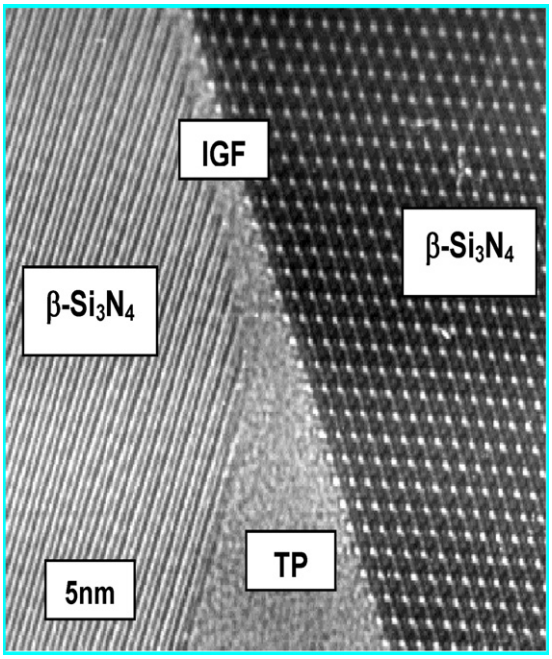

Fig. 2. TEM micrograph of silicon nitride showing a triple point (TP) glass pocket and intergranular glass film (IGF) between two β-Si_3N_4 grains.

silicon nitrides sintered with different amounts and ratios of Y_2O_3:Al_2O_3 to the same level of porosity with the same grain size, both fracture toughness and aspect ratio of the β grains vary with composition in the same way, showing that more elongated rod-like crystals have better resistance to crack propagation.[10] As the grain boundary composition changes, the aspect ratios of β grains vary and grain coarsening also occurs as sintering time or temperature is increased.

Various Ln oxides,[11,12] with either alumina or MgO, have also been investigated as sintering additives for silicon nitride and this allows the development of different types of microstructures and, hence, properties by modifying the chemistry of the sintering liquid phase. Valuable insights can be gained by high resolution transmission electron microscopy (HRTEM) into the nature of the oxynitride glass grain boundaries and, in particular, the nanoscale films which are present at almost all β-Si_3N_4 grain faces[6–8,13] as shown in Fig. 2.[15] The thickness of the IGF is very sensitive to the type of oxide additive used and its concentration and film thickness (in the range 0.5–1.5 nm) depends strongly on chemical composition[6–8,13] but not on the amount of glass present.[8] According to Tanaka et al.,[6] the variation in film thickness can be qualitatively understood in terms of the balance of three long-range forces acting normal to the film, namely the van der Waals dispersion force, a structural "steric" force, and an electrical-doublelayer force. However, Zhang et al.[13] studied the dynamic behaviour of a nanometer-scale amorphous IGF in Si_3N_4 ceramic by an *in situ* heating experiment in a HRTEM in which the IGF gradually vanishes at 820 °C accompanied by the formation of crystal planes in the interface region. The IGF reappears after cooling back to room temperature. They conclude that their results cannot be explained within the framework of a force balance model but put forward alternative explanations

based on low temperature material transport processes that lead to alteration of the IGF composition during annealing.[13]

The overall development of β-Si_3N_4 microstructures during sintering is influenced by the adsorption of Ln cations at silicon nitride grain surfaces[11,12,16] and by the viscosity of the intergranular phases. A model, based on the differential binding energy (DBE), has been developed[16,17] to characterise the competition between Ln atoms and Si as they diffuse to the β-Si_3N_4 grain surfaces. It was predicted that La should have the strongest and Lu the weakest preferential segregation to the grain surfaces of all the lanthanides. Those elements with larger positive DBE values than Si prefer to reside in more oxygen-rich regions while those with negative values have an even higher preference than Si for bonding to nitrogen at the Si_3N_4 grain surfaces. Additional calculations have defined the adsorption sites and their binding strengths for each of the lanthanides on the β-Si_3N_4 prismatic planes. The theoretical work has been combined with aberration-corrected *Z*-contrast scanning transmission electron microscopy (STEM)[18] and unique atomic-resolution images reveal that the lanthanides that induce the greatest observed grain anisotropy are those with the strongest preferential segregation plus high binding strength to the β-Si_3N_4 prismatic grain surface.

2. Oxynitride glass chemistry and properties

As progress was made in understanding the nature of silicon nitride ceramics, how additive chemistry controls microstructure and how microstructure affects properties, there was a growing impetus to understand the nature of these intergranular oxynitride glass phases. This resulted in a number of investigations of oxynitride glass formation, structure, properties and crystallisation in various M–Si–O–N,[19–22] M–Si–Al–O–N[15,19,23–28,30] and M–Si–Mg–O–N[29,30] systems, where M is a modifying cation such as Mg, Ca, Ba, Sc, Y and the lanthanides. Essentially, oxynitride glasses are silicates and alumino-silicates in which nitrogen atoms substitute for oxygen in the glass network.[15,30]

Convenient methods of representing the complex M–Si–Al–O–N systems[31] have been developed. Fig. 3 shows the Y–Si–Al–O–N system represented by Jänecke's triangular prism in which the boundaries of the complete oxynitride glass forming region are outlined.[19] The basal plane of the prism is the Si–Al–O–N square. The addition of a fifth component such as Y, produces a prism with the back right triangular face being a ternary oxide system and the front left face the nitrides. Any point in the prism represents a combination of 12 positive and 12 negative valencies. For a system containing three types of cations, Si, Al and M with valencies of v_{Si}, v_{Al}, and v_M, respectively, in this case, Si^{IV}, Al^{III} and Y^{III}, then:

$$\text{Equivalent percent (equiv.\%) of Si} = \frac{(v_{Si}[Si]) \times 100}{v_{Si}[Si] + v_{Al}[Al] + v_M[M]} \quad (3)$$

$$\text{Equivalent percent (equiv.\%) of Al} = \frac{(v_{Al}[Al]) \times 100}{v_{Si}[Si] + v_{Al}[Al] + v_M[M]} \quad (4)$$

$$\text{Equivalent percent (equiv.\%) of M} = \frac{(v_M[M]) \times 100}{v_{Si}[Si] + v_{Al}[Al] + v_M[M]} \quad (5)$$

where [Si], [Al] and [M] are, respectively, the atomic concentrations of Si, Al and M. If the system also contains two types of anions, O and N with valencies v_O and v_N, respectively, i.e. O^{II}, N^{III}, then:

$$\text{Equivalent percent (equiv.\%) of O} = \frac{(v_O[O]) \times 100}{v_O[O] + v_N[N]} \quad (6)$$

$$\text{Equivalent percent (equiv.\%) of N} = \frac{(v_O[N]) \times 100}{v_O[O] + v_N[N]} \quad (7)$$

It has been shown[25–28] that when cation ratios (M:Si:Al) are kept constant, properties increase with nitrogen addition and linear correlations are typically observed between N content and Young's modulus, microhardness, glass transition temperature, viscosity and microhardness. Each of these changes with increase in nitrogen is a result of (1) the increased anion coordination with Si when N replaces O and (2) the greater resistance to bending of the Si–N–Si bond,[30] which results from the more covalent nature of the Si–N bond compared with the Si–O bond.

Fig. 4 shows a typical plot of Young's modulus as a function of N content for Y–Si–Al–O–N glasses with Y:Si:Al = 37:42:21 (in equiv.%).[32] Elastic modulus is a function of bond energies, network compactness and cross-linking of the glass network and it has been shown that increases in elastic modulus with N can be related to increases in fractional glass compactness and decreases in molar volume.[32,33]

Fig. 5 shows the results of viscosity tests at 950 °C and 1020 °C as a function of N content for Y–Si–Al–O–N glasses with Y:Si:Al = 28:56:16 (in equiv.%). Viscosity increases linearly[32] with nitrogen substitution for oxygen by some 2 orders of magnitude with 18 equiv.% N. This effect is a result of the increase in the rigidity and covalence of the bonding of the

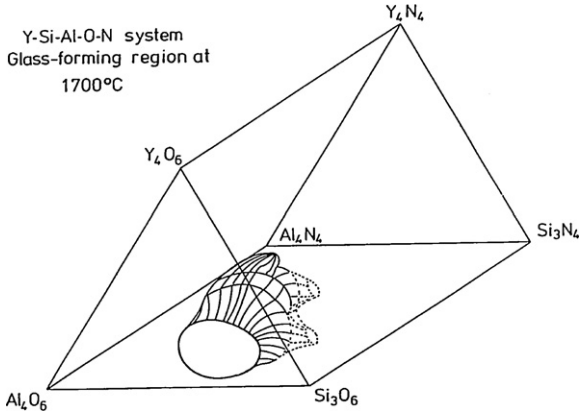

Fig. 3. Jänecke's triangular prism representation of the Y–Si–Al–O–N system showing the oxynitride glass forming region after melting at 1700 °C.[13]

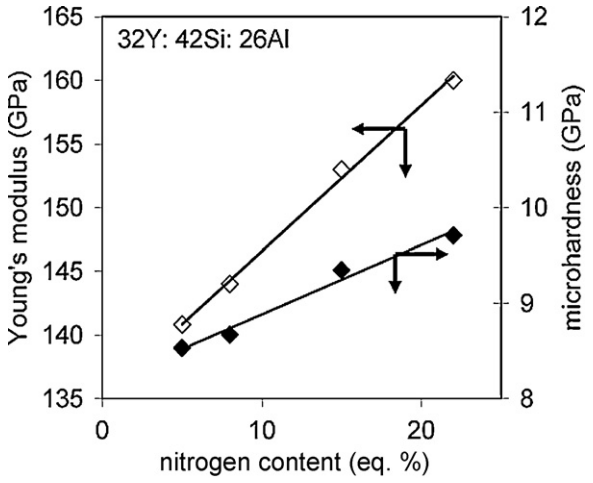

Fig. 4. Effect of nitrogen content on Young's modulus (E) and microhardness (μH_v) for glasses with cation composition (in equiv.%): 37Y:42Si:21Al.

network as nitrogen substitutes for oxygen,[30,32] which inhibits relaxation of the network as the temperature increases.

For Ln–Si–Al–O–N glasses with constant O:N and Ln:Si:Al ratios, evidence shows that as the lanthanide atomic number increases, Young's modulus, hardness, glass transition temperature (T_g) and viscosity increase almost linearly with increases in lanthanide cation field strength,[26,28,30] CFS (where CFS = v/r^2, v is valency and r is ionic radius), which is attributed to increasing compactness of the glass network due to the smaller ions exerting stronger bonding on the $(Si,Al)(O,N)_4$ tetrahedra in the glass structure.[30]

Fig. 6 demonstrates the effects of different Ln cations (Eu, Ce, Sm, Dy, Y, Ho, and Er) on viscosities of Ln–Si–Al–O–N glasses of composition (in equiv.%): 28Ln:56Si:16Al. At any particular temperature, viscosity decreases by ~3 orders of magnitude in the order: Er > Ho ≥ Dy > Y > Sm > Ce > Eu. Viscosities of some Ln–Si–Al–O–N liquids (Sm, Ce, Eu) for a given level of

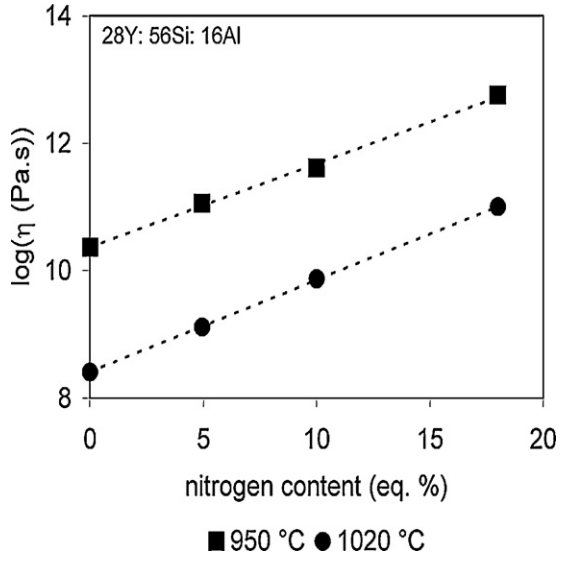

Fig. 5. Effect of nitrogen content on viscosity (at 950 °C and 1020 °C) of Y–Si–Al–O–N glasses with cation composition (in equiv.%): 28Y:56Si:16Al.

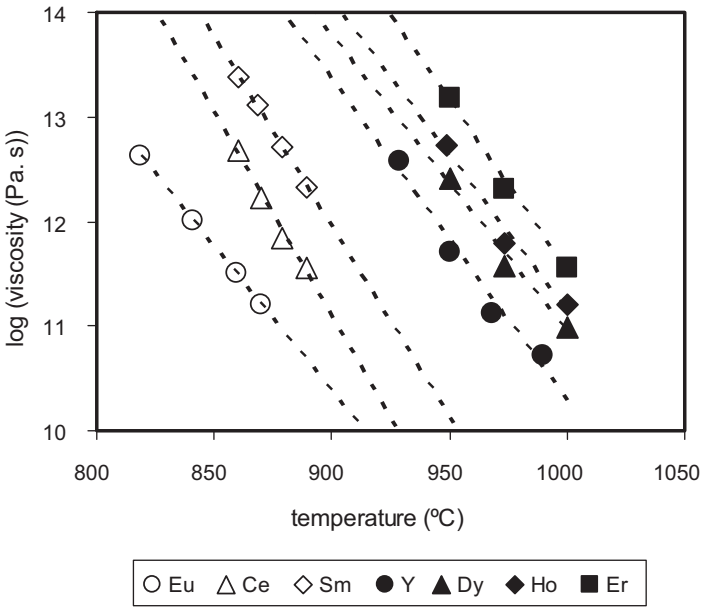

Fig. 6. Viscosities of different Ln–Si–Al–O–N glasses with constant N content and cation composition (in equiv.%): 28Ln:56Si:16Al.

nitrogen are less than those of the equivalent Y–Si–Al–O–N liquids and this should promote easier densification of silicon nitride. In these cases, the ionic radii are larger than that of Y (assuming Eu in 2+ oxidation state).[34] The beneficial effects for sintering are counteracted by the negative consequences for high temperature behaviour, particularly creep resistance. Those cations with ionic radius smaller than Y exhibit higher viscosities and should provide grain boundary glasses with higher creep resistance.

3. Effects of glass chemistry on properties of silicon nitride

It is clear that grain boundary chemistry affects interfacial bond strengths.[7,10–12] One of the critical issues in microstructural design of silicon nitride ceramics is to control the debonding behaviour at the interface between the β-Si_3N_4 grains and the intergranular glassy phase so that the elongated β grains can contribute to toughening mechanisms such as crack deflection and crack bridging. Becher et al.[10] reported significant improvements in the fracture resistance of self-reinforced silicon nitride ceramics by tailoring the chemistry of the intergranular amorphous phase. They found that the steady-state fracture toughness values of these silicon nitrides increased with the Y:Al ratio[10] of the oxide additives as shown in Fig. 7. The increased toughness was accompanied by a steeply rising R-curve and extensive interfacial debonding between the elongated β-Si_3N_4 grains and the intergranular glassy phase. Weaker interfaces, which should be related to lower Young's modulus of the glass, favour higher fracture toughness. Fig. 8 shows the effect of Y:Al ratio on Young's modulus of Y–Si–Al–O–N glasses which decreases with increasing Y:Al ratio, i.e. with easier interfacial de-bonding and increasing K_{Ic} in Si_3N_4. Compared to silicon nitrides

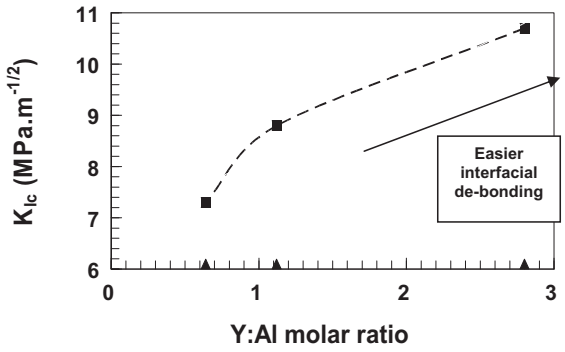

Fig. 7. Fracture toughness of silicon nitride sintered with different Y_2O_3:Al_2O_3 ratios (data from Becher et al.[10]).

with low Y:Al ratios, the high Y:Al ratio materials exhibited more extensive debonding at grain boundary interfaces, resulting in increased intergranular fracture. Microstructural and chemical characterisation reveals that the Y:Al ratios in the additives influence the atomic bonding structure across the β-Si_3N_4/intergranular glass interface by altering the composition of the glassy phase and inducing different Al and O contents in the growth region of the elongated grains. In order to gain further understanding of the influence of intergranular glass on the fracture toughness of silicon nitride, the debonding behaviour of the interface between the prismatic faces of β-Si_3N_4 whiskers and oxynitride glasses was investigated in model systems based on various Si–(Al)–Y(or Ln)–O–N oxynitride glasses.[35] It was found that while the interfacial debonding strength increased when an epitaxial β-SiAlON layer grew on the β-Si_3N_4 rod-like grains, the critical angle for debonding was lowered with increasing Al and O concentrations in the SiAlON layer showing that by tailoring the densification additives, and hence the chemistry of the intergranular glass, it is possible to significantly improve the fracture resistance of silicon nitride.

At temperatures exceeding 1000 °C, strengths decrease due to the softening of the intergranular glass phase. Grain boundary chemistry, effective viscosity and volume fraction of the intergranular glass phase control creep rate and formation and growth of cavities in the amorphous phase.[36] Dynamic microstructural changes occur as the intergranular glass phase goes through its glass transition temperature and at higher temperatures, crystallisation sequences commence which can affect high temperature properties and oxidation.[37] For example, it is well known that Y–Si–O–N quaternary compounds oxidise with a large specific volume expansion leading to microcracking and degradation of the silicon nitride.[31]

Since the intergranular glass is known to have deleterious effects on high-temperature mechanical properties of silicon nitride, these can be improved by decreasing the amount of grain boundary glass through higher pressure processing or by crystallisation of the glass through controlled post-sintering annealing.[38–41]

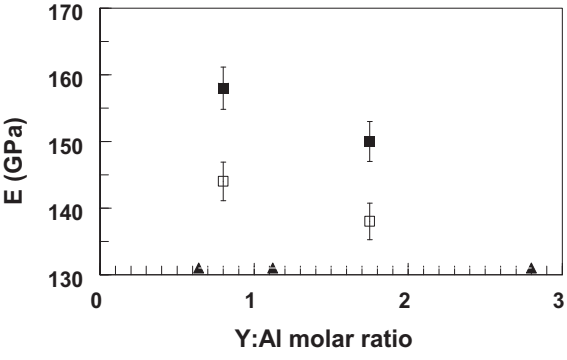

Fig. 8. Young's modulus of Y–Si–Al–O–N glasses with 10 and 20 equiv.% N as a function of Y:Al ratio. Y_2O_3:Al_2O_3 additive ratios for Si_3N_4 shown in Fig. 7 are highlighted.

4. Crystallisation of oxynitride glasses of similar composition to grain boundary glasses in silicon nitride

Crystallisation heat treatments on silicon nitride ceramics can lead to significant improvements in strength particularly at high temperatures (>800 MPa at 1300 °C). Post-sintering heat treatment of Si_3N_4 ceramics densified with the Y_2O_3 and Al_2O_3 results in crystallisation of different yttrium silicates, especially $Y_2Si_2O_7$, from grain boundary glass.[40,41] Sajgalík et al.[42] investigated preformed bulk glasses in the $Y_3Al_5O_{12}$–SiO_2 system with the additions of CaO as model grain boundary phases for Si_3N_4 ceramics. $Y_2Si_2O_7$, was the major crystallisation product but as annealing time increased, Ca-containing aluminosilicates were formed along with cavities within the glasses due to differences in specific volumes of the resulting phases. Other studies of crystallisation[25,43] of bulk Y–Si–Al–O–N glasses in the range 1000–1300 °C show that, once again, yttrium disilicate is a major phase and the morphology changes with temperature. As further growth occurs at longer times or higher temperatures, yttrium aluminium garnet, YAG, also crystallises leaving a N-rich glass phase from which silicon oxynitride precipitates. In general, the crystallisation products depend on both the heat-treatment process and the composition of the parent glass, particularly the cation ratios.

Ramesh et al.[44] used a two-stage glass–ceramic heat treatment process to study the optimisation of nucleation and crystallisation of a glass of composition (in equiv.%): 28Y:56Si:16Al:83O:17N. The major crystalline phases present are mixtures of different forms of yttrium disilicate and silicon oxynitride. Bulk nucleation was observed to be the dominant nucleation mechanism.

In order to determine the optimum nucleation temperature, classical furnace heat treatments were conducted at intervals of 20 °C over a temperature range from $T_g - 40$ to $T_g + 100$ (°C) for 10 h followed by heating to 1270 °C for 30 min to grow the crystal nuclei for subsequent microstructural and microhardness analysis. Having established the optimum nucleation temperature, the optimum nucleation hold time was established by holding the sample for different times prior to heating to 1270 °C for 30 min to grow the crystals. The highest fractional crystallisation as found by microstructural analysis occurred at 1025 °C corresponding to $T_g + 40$ °C which was also the temperature at which microhardness exhibited a maximum with an increase over that for the parent glass of 5.3%. Further heat treatments

were then carried out under these optimum conditions followed by a second heat treatment (crystal growth temperature) varying from 1170 to 1310 °C at 20 °C intervals for 30 min. The temperature which resulted in the highest level of crystallisation and increase in microhardness was 1210 °C ($T_{C3} - 60$ °C) (T_{C3} is the third crystallisation temperature) and this also coincided with the largest increase in microhardness compared with the parent glass of 12.7% at 1210 °C.

Differential thermal analysis, DTA, was also carried out to determine the optimum nucleation temperature according to the method reported by Marotta et al.[45] who concluded that, if samples are held for the same time t_n, at each heat-treatment temperature T_n, then $\ln I$ (kinetic rate constant for nucleation) is proportional to $\{(1/T_p) - (1/T_p')\}$, where T_p and T_p' are, respectively, the crystallisation exotherm temperatures obtained with and without a nucleation hold. Plotting $\{(1/T_p) - (1/T_p')\}$ against nucleation hold temperature gives a bell shaped curve, with the optimum nucleation temperature corresponding to the maximum of this curve. The activation energy (E) is related to heating rate (α) and crystallisation temperature T_p such that a plot of $\ln(\alpha^3/T_p^2)$ versus $1/T_p$ gives a straight line of slope $-3E/R$ (R is gas constant), when crystallisation is a bulk process. The plot of $\{(1/T_p) - (1/T_p')\}$ against nucleation hold temperature[44] showed that optimum nucleation temperature was 1020 °C, i.e. $T_g + 35$ °C, which is in close agreement with the optimum nucleation temperature determined using the heat treatment experiments. The activation energy calculated from the slope of the plot was 834 kJ mol^{-1} which is close to the activation energies observed for viscous flow of Y–Si–Al–O–N glasses, implying that the dominant mechanism is diffusion controlled.

The different nucleation hold temperatures yielded differing phase assemblages. Thus, at $T_g - 40$ °C and $T_g - 20$ °C, yttrium disilicates are the only phases crystallised from the glass, while at higher temperatures silicon oxynitride is also a crystallisation product. At temperatures of $T_g + 20$ °C and above, YAG crystallises in trace amounts. With respect to the yttrium disilicates, the most abundant polymorph changes with nucleation hold temperature. Accordingly, while the α-polymorph is most prevalent over the temperature range $T_g - 40$ °C to $T_g + 20$ °C, the β-polymorph is present in the greatest amounts over the temperature range from $T_g + 40$ °C (the optimum nucleation temperature) to $T_g + 100$ °C.

Following the two-stage treatments, the lowest crystal growth temperature investigated, 1170 °C, showed only y-yttrium disilicate present, strongly suggesting that this is the only polymorph of yttrium disilicate stable at this temperature. y-Yttrium disilicate was also present at 1190 °C but with some α present, indicating that this latter polymorph becomes more stable at this crystallisation temperature. 1210 °C is the crystal growth temperature at which the highest fraction crystallised and greatest improvement in microhardness was found and corresponds to a phase assemblage comprising α- and β-yttrium disilicates. At 1220 °C, in addition to the α- and β-yttrium disilicates, traces of both silicon oxynitride and YAG appear. The oxynitride becomes more prevalent at higher crystal growth temperatures of 1290 and 1310 °C at which the most stable yttrium disilicate is the δ-polymorph.

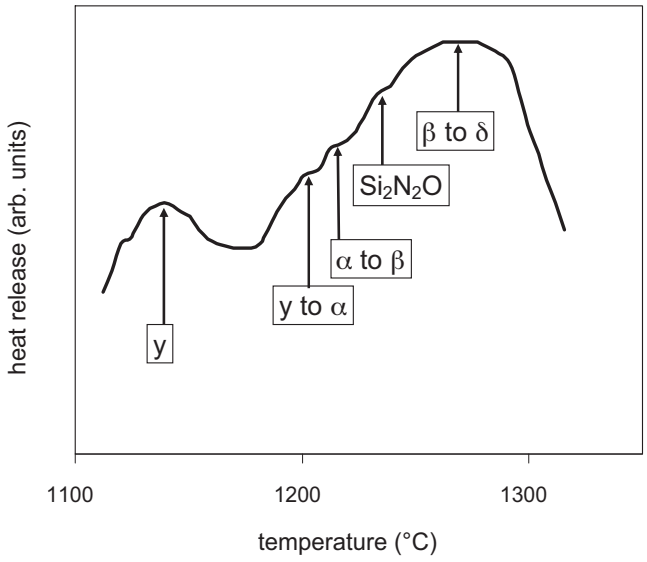

Fig. 9. DTA curve showing crystallisation events in glass with composition (in equiv.%): 28Y:56Si:16Al:83O:17N for different $Y_2Si_2O_7$ polymorphs and Si_2N_2O as a function of temperature.[46]

As a result of these observations of these multi-phase products of nucleation and crystal growth, a further analysis of the DTA curve was undertaken.[46] Fig. 9 is a reinterpretation of the original curve and shows the positions of the crystallisation of y-yttrium disilicate and the y- to α-$Y_2Si_2O_7$, α- to β-$Y_2Si_2O_7$ and β- to δ-$Y_2Si_2O_7$ transformations. It is clear that the discontinuities in the curve can be associated with these transformations and the crystallisation of Si_2N_2O. Crystallisation of this Y–Si–Al–O–N glass is not a simple devitrification process but also involves various phase transformations which allow the microstructural changes needed to achieve the optimum degree of crystallisation and increase in microhardness. In a system where polymorphic changes arise during heat treatment then optimum nucleation conditions determined by both heat treatment and DTA studies may relate only to the best heterogeneous nucleation conditions for microstructural development through both crystal growth and phase transformation. This may be problematic for silicon nitride ceramics where the temperature of operation may differ from that used to crystallise the grain boundary glass.

An alternative approach is to stabilise one polymorph of the disilicate by replacing 25 at.% of Y by La. Pomeroy et al.[47] showed that a single α-$Y_2Si_2O_7$ phase could be obtained on heating a mixed Y–La–Si–Al–O–N glass with composition (in equiv.%): 21Y:7La:56Si:16Al:83O:17N to 1300 °C. This should be expected when taking into consideration the average ionic radius for the mixed La and Y glass modifiers and superimposing this on the disilicate polymorph stability – ionic radius map given by Liddell and Thompson[48] according to which the mixed α-$Y_{1.5}La_{0.5}Si_2O_7$ should be stable up to at least 1350 °C before any transformation occurs.

5. Summary

(1) Oxide sintering additives such as yttrium oxide or lanthanide oxides plus alumina provide conditions for liquid phase

densification of silicon nitride following which the liquid remains as an intergranular oxynitride glass.

(2) As nitrogen is substituted for oxygen in these oxynitride glasses increases in elastic modulus, hardness, glass transition temperature and viscosity are observed because nitrogen introduces extra cross-linking into the glass network compared with the equivalent oxide glass with the same cation composition. These properties also increase with increasing cation field strength of the lanthanide modifier for fixed oxygen:nitrogen ratio.

(3) In silicon nitride ceramics, the amounts and ratios of the additives initially introduced determine the quantity and chemistry of the glass phase and this affects properties such as fracture toughness, ambient and high temperature strengths, creep resistance and oxidation resistance. Significant improvements in fracture resistance of self-reinforced silicon nitride ceramics can be achieved by tailoring the chemistry (Y or Ln):Al ratio of the intergranular amorphous phase. Weaker interfaces, which should be related to lower Young's modulus of the glass, favour higher fracture toughness. The choice of lanthanide modifier is essential to optimise microstructure, interfacial debonding and mechanical properties.

(4) Grain boundary glass chemistry, effective viscosity and volume fraction of the intergranular glass phase control creep rate and behaviour of silicon nitride ceramics at high temperatures. Crystallisation of the grain boundary glass phase is one approach to improving properties. The crystal transformations occurring during a two-stage nucleation-and-growth treatment for a Y-SiAlON glass containing 17 equiv.% N can be optimised. The crystallisation of these glasses is highly complex due to the fact that all 5 polymorphs of yttrium disilicate can form under varying conditions of heat treatment as well as the additional crystallisation of silicon oxynitride.

(5) The devitrification processes in Y–Si–Al–O–N glasses can be simplified by substituting Y by a lanthanide ion such that the average ionic radius of the mixed modifier system is compatible with crystallisation of a single Y–La disilicate polymorph.

References

1. Riley FL. Silicon nitride and related materials. *J Am Ceram Soc* 2000;**83**(2):245–65.
2. Lange FF. The sophistication of ceramic science through silicon nitride studies. *J Ceram Soc Jpn* 2006;**114**:873–9.
3. Hampshire S. The role of additives in the pressureless sintering of nitrogen ceramics. *Metals Forum* 1984;**7**:162–8.
4. Hampshire S, Jack KH. The kinetics of densification and phase transformation in nitrogen ceramics. *Proc Brit Ceram Soc* 1981;**31**:37–49.
5. Mandal H. New developments in α-SiAlON ceramics. *J Eur Ceram Soc* 1999;**19**:2349–57.
6. Tanaka I, Kleebe H-J, Cinibulk MK, Bruley J, Clarke DR, Rühle M. Calcium concentration dependence of the intergranular film thickness in silicon nitride. *J Am Ceram Soc* 1994;**77**(4):911–4.
7. Kleebe H-J, Pezzotti G, Ziegler G. Microstructure and fracture toughness of Si_3N_4 ceramics: combined roles of grain morphology and secondary phase chemistry. *J Am Ceram Soc* 1999;**82**(7):1857–67.
8. Wang CM, Pan WQ, Hoffmann MJ, Cannon RM, Rühle M. Grain boundary films in rare-earth-glass-based silicon nitride. *J Am Ceram Soc* 1996;**79**(3):788–92.
9. Becher PF, Sun EY, Plucknett KP, Alexander KB, Hsueh C-H, Lin H-T, et al. Microstructural design of silicon nitride with improved fracture toughness: I. Effects of grain size and shape. *J Am Ceram Soc* 1998;**81**(11):2821–30.
10. Sun EY, Becher PF, Plucknett KP, Hsueh C-H, Alexander KB, Waters SB, et al. Microstructural design of silicon nitride with improved fracture toughness: II. Effects of yttria and alumina additives. *J Am Ceram Soc* 1998;**81**(11):2831–40.
11. Satet RL, Hoffmann MJ, Cannon RM. Experimental evidence of the impact of rare-earth elements on particle growth and mechanical behaviour of silicon nitride. *Mater Sci Eng A* 2006;**422**:66–76.
12. Becher PF, Shibata N, Painter GS, Averill F, van Benthem K, Lin H-T, et al. Observations on the influence of secondary Me oxide additives (Me = Si, Al, Mg) on the microstructural evolution and mechanical behavior of silicon nitride ceramics containing RE_2O_3 (RE = La, Gd, Lu). *J Am Ceram Soc* 2010;**93**(2):570–80.
13. Zhang Z, Sigle W, Koch CT, Rühle M. Dynamic behavior of nanometer-scale amorphous intergranular film in silicon nitride by *in situ* high-resolution transmission electron microscopy. *J Eur Ceram Soc* 2011;**31**:1835–40.
14. Kingery WD. Densification during sintering in the presence of a liquid phase I. Theory. *J Appl Phys* 1959;**30**:301–6.
15. Hampshire S, Pomeroy MJ. Oxynitride glasses. *Int J Appl Ceram Tech* 2008;**5**(2):155–63.
16. Painter GS, Averill F, Becher PF, Shibata N, van Benthem K, Pennycook SJ. First-principles study of rare earth adsorption at β-Si_3N_4 interfaces. *Phys Rev B* 2008;**78**:214206.
17. Becher PF, Painter GS, Shibata N, Satet RL, Hoffmann MJ, Pennycook SJ. Influence of additives on anisotropic grain growth in silicon nitride ceramics. *Mater Sci Eng A* 2006;**422**:85–91.
18. Shibata N, Pennycook SJ, Gosnell TR, Painter GS, Shelton WA, Becher PF. Observation of rare earth segregation in silicon nitride ceramics at sub-nanometer dimensions. *Nature* 2004;**428**:730–3.
19. Hampshire S, Drew RAL, Jack KH. Oxynitride glasses. *Phys Chem Glass* 1985;**26**:182–6.
20. Ohashi M, Hampshire S. Formation of Ce–Si–O–N glasses. *J Am Ceram Soc* 1991;**74**(8):2018–20.
21. Ohashi M, Nakamura K, Hirao K, Kanzaki S, Hampshire S. Formation and properties of Ln–Si–O–N glasses. *J Am Ceram Soc* 1995;**78**:71–6.
22. Hakeem AS, Dauce R, Leonova E, Eden M, Shen Z, Grins J, et al. Silicate glasses with unprecedented high nitrogen and electropositive metal contents obtained by using metals as precursors. *Adv Mater* 2005;**17**:2214–6.
23. Loehman RE. Preparation and properties of yttrium–silicon–aluminum oxynitride glasses. *J Am Ceram Soc* 1979;**62**(9–10):491–4.
24. Sakka S, Kamiya K, Yoko T. Preparation and properties of Ca–Al–Si–O–N oxynitride glasses. *J Non-Cryst Solids* 1983;**56**:147–55.
25. Hampshire S, Nestor E, Flynn R, Besson J-L, Rouxel T, Lemercier H, et al. Yttrium oxynitride glasses: properties and potential for crystallisation to glass–ceramics. *J Euro Ceram Soc* 1994;**14**:261–73.
26. Ramesh R, Nestor E, Pomeroy MJ, Hampshire S. Formation of Ln–Si–Al–O–N glasses and their properties. *J Eur Ceram Soc* 1997;**17**:1933–9.
27. Sun EY, Becher PF, Hwang S-L, Waters SB, Pharr GM, Tsui TY. Properties of silicon–aluminum–yttrium oxynitride glasses. *J Non-Cryst Solids* 1996;**208**:162–9.
28. Becher PF, Waters SB, Westmoreland CG, Riester L. Influence of composition on the properties of SiREAl oxynitride glasses: RE = La, Nd, Gd, Y, or Lu. *J Am Ceram Soc* 2002;**85**(4):897–902.
29. Lofaj F, Deriano S, LeFloch M, Rouxel T, Hoffmann MJ. Structure and rheological properties of the RE–Si–Mg–O–N (RE = Sc, Y, La, Nd, Sm, Gd, Yb and Lu) glasses. *J Non-Cryst Solids* 2004;**344**:8–16.
30. Becher PF, Hampshire S, Pomeroy MJ, Hoffmann MJ, Lance M, Satet RL. An overview of the structure and properties of silicon-based oxynitride glasses. *Int J Appl Glass Sci* 2011;**2**(1):63–83.
31. Jack KH. Review: SiAlONs and related nitrogen ceramics. *J Mater Sci* 1976;**11**:1135–58.

32. Pomeroy MJ, Hampshire S. SiAlON glasses: effects of nitrogen on structure and properties. *J Ceram Soc Jpn* 2008;**116**:755–61.
33. Rouxel T. Elastic properties and short-to-medium-range order in glasses. *J Am Ceram Soc* 2007;**90**(10):3019–39.
34. Hampshire S. Oxynitride glasses. *J Eur Ceram Soc* 2008;**28**(7):1475–83.
35. Sun EY, Becher PF, Hsueh C-H, Painter GS, Waters SB, Hwang S-L, et al. *Acta Mater* 1999;**47**(9):2777–85.
36. Luecke WE, Widerhorn SM, Hockey BJ, Krause RF, Long GG. Cavitation contributes substantially to tensile creep in silicon nitride. *J Am Ceram Soc* 1995;**78**(8):2085–96.
37. Rouxel T. High temperature mechanical behavior of silicon nitride ceramics. *J Ceram Soc Jpn* 2001;**109**:S89–97.
38. Falk LKL, Dunlop G. Crystallization of the glassy phase in an Si_3N_4 material by post-sintering heat treatments. *J Mater Sci* 1987;**22**:4369–76.
39. Tsuge A, Inoue H, Komeya K. Grain-boundary-phase crystallisation and strength of silicon nitride with material loss during heat treatment. *J Am Ceram Soc* 1989;**72**:2014–6.
40. Cinibulk MK, Thomas G. Fabrication and secondary-phase crystallisation of rare-earth disilicate-silicon nitride ceramics. *J Am Ceram Soc* 1992;**75**:2037–43.
41. Bernard-Granger G, Crampon J, Duclos R, Cales B. Glassy grain boundary phase crystallisation of silicon nitride: kinetics and phase development. *J Mater Sci Lett* 1995;**14**:1362–5.
42. Lichvár P, Sajgalík P, Liška M, Galusek D. CaO–SiO_2–Al_2O_3–Y_2O_3 glasses as model grain boundary phases for Si_3N_4 ceramics. *J Eur Ceram Soc* 2007;**27**:429–36.
43. Besson J-L, Billieres D, Rouxel T, Goursat P, Flynn R, Hampshire S. Crystallization and properties of a Si–Y–Al–O–N glass ceramic. *J Am Ceram Soc* 1993;**76**(8):2103–5.
44. Ramesh R, Nestor E, Pomeroy MJ, Hampshire S. Classical and DTA studies of the glass–ceramic transformation in a YSiAlON glass. *J Am Ceram Soc* 1998;**81**(5):1285–97.
45. Marotta A, Buri A, Branda F, Saiello S. Nucleation and crystallisation of $Li_2O{\cdot}2SiO_2$ glass – a DTA study. In: Simmons JH, Uhlmann DR, Beall BH, editors. *Advances in ceramics, vol. 4, nucleation and crystallization in glasses*. Columbus, OH, USA: American Ceramic Society; 1982. p. 146–52.
46. Pomeroy MJ, Hampshire S. Controlled crystallisation of a Y–Si–Al–O–N glass typical of grain boundary glasses formed in silicon nitride-based ceramics. *J Ceram Soc Jpn* 2008;**116**:722–6.
47. Pomeroy MJ, Nestor E, Ramesh R, Hampshire S. Properties and crystallisation of rare earth SiAlON glasses containing mixed trivalent modifiers. *J Am Ceram Soc* 2005;**88**(4): 875–81.
48. Liddell K, Thompson DP. X-ray diffraction data for yttrium disilicates. *Br Ceram Trans J* 1986;**85**:17–22.